

Numerical solution of the linear dispersion relation in a relativistic pair plasma

J Pétri and J G Kirk

Max-Planck-Institut für Kernphysik, Saupfercheckweg 1, 69117 Heidelberg, Germany

E-mail: j.petri@mpi-hd.mpg.de

Abstract. We describe an algorithm that computes the linear dispersion relation of waves and instabilities in relativistic plasmas within a Vlasov-Maxwell description. The method used is fully relativistic and involves explicit integration of particle orbits along the unperturbed equilibrium trajectories. We check the algorithm against the dispersion curves for a single component magnetised plasma and for an unmagnetised plasma with counter-streaming components in the non-relativistic case. New results on the growth rate of the Weibel or two-stream instability in a hot unmagnetised pair plasma consisting of two counter-streaming relativistic Maxwellians are presented. These are relevant to the physics of the relativistic plasmas found in gamma-ray bursts, relativistic jets and pulsar winds.

PACS numbers: 52.27.Ny; 52.35.-g; 95.30.Qd

Submitted to: *Plasma Phys. Control. Fusion*

1. Introduction

Relativistic shock fronts and currents sheets in relativistic flows play an important role in astrophysical models of gamma-ray bursts (for a review see Piran [1]), of jets and of pulsar winds (see for instance Michel [2] and Kirk [3]). The underlying plasma is probably composed of electrons, positrons and protons, whose temperature may be relativistic, i.e. comparable to their rest mass energy.

We present an algorithm that computes the linear dispersion relation of waves in such plasmas within a Vlasov-Maxwell description. The method used is based on that presented by Daughton [4] for non relativistic Maxwellians, and involves explicit time integration of particle orbits along the unperturbed trajectories. We modify and extend this method by changing the manner in which the roots of the dispersion relation are located and adopt a fully relativistic approach, i.e. relativistic temperatures as well as relativistic drift speeds.

Particular emphasis is given to the two-stream or Weibel instability [5]. This instability is very important in astrophysical processes because it is able to generate a magnetic field by pumping free energy from the anisotropic momentum distribution of an unmagnetised plasma or from the kinetic drift energy. There is an extensive literature about the Weibel instability. Although the dispersion curves has been found in some special cases such as, for example a water-bag distribution function, (Yoon [6]), or a fully relativistic bi-Maxwellian distribution function, (Yoon [7]), looking for an analytical expression for the dispersion relation for a given equilibrium distribution function is a complicated or even impossible task. The water-bag distribution is also the preferred profile to analyse magnetic field generation in fast ignitor scenarios, (Silva et al. [8]) or in relativistic shocks, (Wiersma and Achterberg [9], Lyubarsky and Eichler [10]). The Weibel instability in a magnetised electron-positron pair plasma has been investigated by Yang et al [11] for the water-bag and for a smooth distribution function and a covariant description has been formulated by Melrose [12] and by Schlickeiser [13]. General conditions for the existence of the relativistic Weibel instability for arbitrary distribution functions are discussed in [14]. Wave propagation in counter-streaming magnetised nonrelativistic Maxwellian plasmas are studied in [15, 16]. The stability properties of a nonrelativistic Harris current sheet have been studied by Daughton [4] and also by Silin et al. [17]. Streaming instabilities in relativistic magnetised plasmas and superluminous wave propagation are discussed by Buti [18, 19].

In this paper, we investigate the relativistic Weibel instability for two counter-streaming Maxwellian distribution functions in an unmagnetised pair plasma. Our approach follows that of Zelenyi et al. [20], who studied the tearing mode instabilities in a relativistic Harris current sheet, by integrating first order perturbations of the relativistic Maxwellian distribution function along unperturbed particle trajectories. Our algorithm is compared and checked against the dispersion curves for a single component magnetised plasma and for an unmagnetised plasma with counter-streaming components in the non-relativistic case. We present results for the growth rate of the Weibel instability in a

hot unmagnetised pair plasma consisting of counter-streaming relativistic Maxwellians.

The paper is organised as follows. In Sec. 2, we present the full set of non-linear equations governing the motion in the pair plasma and describe the equilibrium of the two counter-streaming relativistic Maxwellians. Next, in Sec. 3, the full set of linearised Vlasov-Maxwell equations for the perturbed electromagnetic potentials around the equilibrium state are presented. The eigenvalue problem and the algorithm are discussed in Sec. 4. Results for magnetised plasma wave oscillations and for the non-relativistic Weibel instability as well as for the relativistic Weibel instability are shown in Sec. 5. Conclusions are drawn in Sec. 6.

2. Equilibrium

Our purpose is to study the Weibel instability in a relativistic plasma. This plasma is made of counter-streaming electrons and positrons with relativistic temperatures and evolving in a static external magnetic field aligned with the z-axis such that

$$\vec{B}_0 = B_0(x) \vec{e}_z \quad (1)$$

In equilibrium, there is no electric field, $\vec{E}_0 = \vec{0}$ and the charges drift in the y direction at a relativistic velocity $\pm U_s$, (+ for positrons and $-$ for electrons with $U_s > 0$). We use Cartesian coordinates, denoted by (x, y, z) , and the corresponding basis $(\vec{e}_x, \vec{e}_y, \vec{e}_z)$. The distribution function at equilibrium for each species "s", denoted by $f_{0s}(\vec{r}, \vec{p})$, is assumed to be a relativistic Maxwellian with drift speed $\pm U_s$. Adopting the usual notations, namely $t, \vec{r}, \vec{v}, \vec{p}, m_s, q_s$ for respectively the time, position, 3-velocity, 3-momentum, mass and charge of a particle of species s, the stationary distribution function reads :

$$f_{0s}(\vec{r}, \vec{p}) = \frac{n_{0s}(\vec{r})}{4\pi m_s^3 c^3 \Theta_s K_2(1/\Theta_s)} \exp[-\Gamma_s (E - U_s p_y)/\Theta_s m_s c^2] \quad (2)$$

$n_{0s}(\vec{r})$ is the particle number density, E the total energy of a particle, p_y the y-component of its momentum, c the speed of light, $\Gamma_s = 1/\sqrt{1 - U_s^2/c^2}$ the Lorentz factor associated with the drift motion and K_2 the modified Bessel function of the second kind. The temperature of the gas is normalised to the rest mass energy of the leptons such that

$$\Theta_s = \frac{k_B T_s}{m_s c^2} \quad (3)$$

and k_B is the Boltzmann constant. We introduce the standard electromagnetic scalar and vector potentials (ϕ, \vec{A}) , related to the electromagnetic field (\vec{E}, \vec{B}) by :

$$\vec{E} = -\vec{\nabla}\phi - \frac{\partial \vec{A}}{\partial t} \quad (4)$$

$$\vec{B} = \vec{\nabla} \wedge \vec{A} \quad (5)$$

We employ the Lorenz gauge condition by imposing

$$\text{div } \vec{A} + \varepsilon_0 \mu_0 \frac{\partial \phi}{\partial t} = 0 \quad (6)$$

with $\varepsilon_0 \mu_0 c^2 = 1$. The relation between potentials and sources then reads :

$$\Delta\phi - \frac{1}{c^2} \frac{\partial^2 \phi}{\partial t^2} + \frac{\rho}{\varepsilon_0} = 0 \quad (7a)$$

$$\Delta\vec{A} - \frac{1}{c^2} \frac{\partial^2 \vec{A}}{\partial t^2} + \mu_0 \vec{j} = 0 \quad (7b)$$

The source terms represented by the charge ρ and current \vec{j} densities, are expressed in terms of the distribution functions by :

$$\rho(\vec{r}, t) = \sum_s q_s \iiint f_s(\vec{r}, \vec{p}, t) d^3\vec{p} \quad (8a)$$

$$\vec{j}(\vec{r}, t) = \sum_s q_s \iiint \frac{\vec{p}}{\gamma m_s} f_s(\vec{r}, \vec{p}, t) d^3\vec{p} \quad (8b)$$

where $\gamma = \sqrt{1 + p^2/m_s^2 c^2}$ is the Lorentz factor of a particle. The time evolution of the distribution functions f_s is governed by the well-known relativistic Vlasov-Maxwell equations written for each species :

$$\frac{\partial f_s}{\partial t} + \vec{v} \cdot \frac{\partial f_s}{\partial \vec{r}} + q_s (\vec{E} + \vec{v} \wedge \vec{B}) \cdot \frac{\partial f_s}{\partial \vec{p}} = 0 \quad (9)$$

The self-consistent non-linear evolution of the plasma is entirely determined by the set of equations (4)-(9).

3. Linearisation

Our next step is to investigate the stability properties of the equilibrium configuration given in (2). The Vlasov equation (9) is linearised for each species about the equilibrium state f_{0s} , (2), to obtain the time evolution of the first order perturbation as

$$\frac{df_{1s}}{dt} = -q (\vec{E}_1 + \vec{v} \wedge \vec{B}_1) \cdot \frac{\partial f_{0s}}{\partial \vec{p}} \quad (10)$$

Perturbations are denoted by the subscript 1 whereas the equilibrium quantities are depicted by a subscript 0. The total time derivative d/dt is to be taken along the trajectories of the particles in the unperturbed electromagnetic field ($\vec{E}_0 = \vec{0}, \vec{B}_0$). More explicitly, performing the time integration in (10), the perturbed distribution function is given by

$$f_{1s}(\vec{r}, \vec{p}, t) = -q \int_{-\infty}^t \left[\vec{E}_1(\vec{r}', t') + \vec{v}' \wedge \vec{B}_1(\vec{r}', t') \right] \cdot \frac{\partial f_{0s}}{\partial \vec{p}}(\vec{r}', \vec{p}') dt' \quad (11)$$

We assume that the perturbation of the distribution function at initial time vanishes, i.e., $f_{1s}(\vec{r}, \vec{p}, t = -\infty) = 0$. Position and momentum are determined by solving the equations of motion for a single particle in the unperturbed electromagnetic field ($\vec{E}_0 = \vec{0}, \vec{B}_0$). Thus, the unperturbed trajectories are solutions of the following system of ordinary differential equations

$$\frac{d\vec{r}'}{dt'} = \vec{v}'(t') \quad (12a)$$

$$\frac{d\vec{p}'}{dt'} = q \vec{v}'(t') \wedge \vec{B}_0(\vec{r}', t') \quad (12b)$$

with initial conditions $\vec{r}'(t' = t) = \vec{r}$ and $\vec{p}'(t' = t) = \vec{p}$. Note also that for the relativistic Maxwellian, (2), we have

$$\frac{\partial f_{0s}}{\partial \vec{p}} = -\frac{\Gamma_s f_{0s}}{k_B T_s} (\vec{v} - U_s \vec{e}_y) \quad (13)$$

Expanding all physical scalar quantities ψ in terms of plane waves with complex frequency ω and real wavenumber vector \vec{k} contained in the plane (yOz)

$$\psi(\vec{r}, t) = \psi(x) \exp(i(k_y y + k_z z - \omega t)) \quad (14)$$

we arrive by standard techniques at expressions for the charge density and current density

$$\begin{aligned} \rho(\vec{r}, t) = \sum_s \frac{\Gamma_s \omega_{ps}^2(\vec{r}) \varepsilon_0}{\Theta_s c^2} [U_s A_y(\vec{r}, t) - \phi(\vec{r}, t) + i(\omega - k_y U_s) \times \\ \times \iiint \hat{f}_{0s}(\vec{r}, \vec{p}) \int_{-\infty}^{\tau(t)} \left(\frac{\vec{p}'}{m_s} \cdot \vec{A}(\vec{r}', \tau') - \gamma' \phi(\vec{r}', \tau') \right) d\tau' d^3\vec{p}] \end{aligned} \quad (15a)$$

$$\begin{aligned} \vec{j}(\vec{r}, t) = \sum_s \frac{\Gamma_s \omega_{ps}^2(\vec{r}) \varepsilon_0}{\Theta_s c^2} \left[(U_s A_y(\vec{r}, t) - \phi(\vec{r}, t)) \iiint \frac{\vec{p} c^2}{E} \hat{f}_{0s}(\vec{r}, \vec{p}) d^3\vec{p} + \right. \\ \left. + i(\omega - k_y U_s) \iiint \frac{\vec{p} c^2}{E} \hat{f}_{0s}(\vec{r}, \vec{p}) \times \right. \\ \left. \times \int_{-\infty}^{\tau(t)} \left(\frac{\vec{p}'}{m_s} \cdot \vec{A}(\vec{r}', \tau') - \gamma' \phi(\vec{r}', \tau') \right) d\tau' d^3\vec{p} \right] \end{aligned} \quad (15b)$$

where the Lorentz factor of an unperturbed trajectory is $\gamma' = \sqrt{1 + p'^2/m_s^2 c^2}$. Liouville's theorem

$$\hat{f}_{0s}(\vec{r}'(\tau'), \vec{p}'(\tau'), \tau') = \hat{f}_{0s}(\vec{r}, \vec{p}) \quad (16)$$

stating that \hat{f}_{0s} is constant along the unperturbed trajectories defined below by (17a) and (17b), was used to extract \hat{f}_{0s} from the final integration over τ' . To compute the integrals, it is more convenient to use the proper time defined by $d\tau' = dt'/\gamma'$. This relation between proper and observer time also defines the limit of time integration $\tau(t)$. The (non-relativistic) plasma frequency corresponding to species "s" is $\omega_{ps}^2 = n_{0s} q_s^2/m_s \varepsilon_0$ and the normalised distribution function is defined by $f_{0s} = n_{0s} \hat{f}_{0s}$. The trajectories are integrated over the unperturbed orbits, in the proper frame, following the equations of motion (12a), (12b):

$$\frac{d\vec{r}'}{d\tau'} = \frac{\vec{p}'(\tau')}{m_s} \quad (17a)$$

$$\frac{d\vec{p}'}{d\tau'} = \vec{p}'(\tau') \wedge \vec{\omega}_{Bs}(\vec{r}') \quad (17b)$$

with initial conditions $\vec{r}'(\tau' = \tau) = \vec{r}$ and $\vec{p}'(\tau' = \tau) = \vec{p}$. The non-relativistic cyclotron frequency is given by $\vec{\omega}_{Bs} = q_s \vec{B}_0/m_s$. According to equation (17a) and (17b), both

energy γ' and momentum component p'_z are conserved so that the equations of motion in the z-direction can be integrated analytically:

$$z'(\tau') = z_0 + p_z \tau' / m_s \quad (18a)$$

$$p'_z(\tau') = p_z = \text{constant} \quad (18b)$$

Consequently, the p_z integration in (15a) and (15b) can be factored out and performed separately. After some algebraic manipulations, the charge density is expressed as

$$\begin{aligned} \rho(x) = \sum_s \frac{n_{0s} q_s^2 \Gamma_s}{k_B T_s} [-\phi(x) + i(\omega - k_y U_s) \times \\ \times \iint_{R^2} \hat{F}_{0s}(x, p_x, p_y) S_\phi(x, p_x, p_y) dp_x dp_y] \end{aligned} \quad (19a)$$

and the current density as

$$\begin{aligned} j_x(x) = \sum_s \frac{n_{0s} q_s^2 \Gamma_s}{k_B T_s} i(\omega - k_y U_s) \times \\ \times \iint_{R^2} \frac{p_x}{m_s} \hat{F}_{0s}(x, p_x, p_y) S_j(x, p_x, p_y) dp_x dp_y \end{aligned} \quad (19b)$$

$$\begin{aligned} j_y(x) = \sum_s \frac{n_{0s} q_s^2 \Gamma_s}{k_B T_s} [\Gamma_s U_s^2 A_y(x) + i(\omega - k_y U_s) \times \\ \times \iint_{R^2} \frac{p_y}{m_s} \hat{F}_{0s}(x, p_x, p_y) S_j(x, p_x, p_y) dp_x dp_y] \end{aligned} \quad (19c)$$

$$\begin{aligned} j_z(x) = \sum_s \frac{n_{0s} q_s^2 \Gamma_s}{k_B T_s} i(\omega - k_y U_s) \times \\ \times \iint_{R^2} \hat{F}_{0s}(x, p_x, p_y) S_{j_z}(x, p_x, p_y) dp_x dp_y \end{aligned} \quad (19d)$$

For brevity, we introduced the following functions :

$$\hat{F}_{0s}(x, p_x, p_y) = \frac{\exp(\Gamma_s U_s p_y / \Theta_s m_s c^2)}{4 \pi m_s^3 c^3 \Theta_s K_2(1/\Theta_s)} \quad (20a)$$

$$S_\phi(x, p_x, p_y) = \int_0^{-\infty} \left\{ \phi' I_{\rho_\phi} - \left[(p'_x A'_x + p'_y A'_y) \frac{I_{\rho_1}}{m_s} + A'_z I_{\rho_{A_z}} \right] \right\} e^{i \vec{k} \cdot \vec{r}'} d\tau' \quad (20b)$$

$$S_j(x, p_x, p_y) = \int_0^{-\infty} \left\{ \phi' I_{\rho_1} - \left[(p'_x A'_x + p'_y A'_y) \frac{I_{j_{A_1}}}{m_s} + A'_z I_{j_{A_2}} \right] \right\} e^{i \vec{k} \cdot \vec{r}'} d\tau' \quad (20c)$$

$$S_{j_z}(x, p_x, p_y) = \int_0^{-\infty} \left\{ \phi' I_{\rho_{A_z}} - \left[(p'_x A'_x + p'_y A'_y) \frac{I_{j_{A_2}}}{m_s} + A'_z I_{j_{A_3}} \right] \right\} e^{i \vec{k} \cdot \vec{r}'} d\tau' \quad (20d)$$

We employ a short-hand notation for $(\phi', A'_x, A'_y, A'_z)$ which should be understood as the scalar and vector potential evaluated at (\vec{r}', τ') on the unperturbed trajectories (17a) and (17b). We also use the following relation for the relativistic Maxwellian (2)

$$\iiint \frac{\vec{p} c^2}{E} \hat{f}_{0s} d^3 \vec{p} = \Gamma_s c \vec{\beta}_s \quad (21)$$

It is easy to show that the proper time integration along the unperturbed orbits in the z direction, (18a) and (18b), leads to expressions involving modified Bessel functions of the second kind K_0 , K_1 and K_2 such that

$$I_{\rho_1} = m_s c \gamma_{\perp} \left(\sqrt{\frac{\beta}{\alpha}} + \sqrt{\frac{\alpha}{\beta}} \right) K_1(2 \sqrt{\alpha \beta}) \quad (22a)$$

$$I_{\rho_{\phi}} = m_s c \gamma_{\perp}^2 \left[K_0(2 \sqrt{\alpha \beta}) + \frac{1}{2} \left(\frac{\beta}{\alpha} + \frac{\alpha}{\beta} \right) K_2(2 \sqrt{\alpha \beta}) \right] \quad (22b)$$

$$I_{\rho_{A_z}} = m_s c^2 \gamma_{\perp}^2 \frac{1}{2} \left(\frac{\beta}{\alpha} - \frac{\alpha}{\beta} \right) K_2(2 \sqrt{\alpha \beta}) \quad (22c)$$

$$I_{j_{A_1}} = 2 m_s c K_0(2 \sqrt{\alpha \beta}) \quad (22d)$$

$$I_{j_{A_2}} = m_s c^2 \gamma_{\perp} \left(\sqrt{\frac{\beta}{\alpha}} - \sqrt{\frac{\alpha}{\beta}} \right) K_1(2 \sqrt{\alpha \beta}) \quad (22e)$$

$$I_{j_{A_3}} = m_s c^3 \gamma_{\perp}^2 \left[\frac{1}{2} \left(\frac{\beta}{\alpha} + \frac{\alpha}{\beta} \right) K_2(2 \sqrt{\alpha \beta}) - K_0(2 \sqrt{\alpha \beta}) \right] \quad (22f)$$

The argument of the modified Bessel functions for wave propagation along \vec{e}_z ($\vec{k} = k_z \vec{e}_z$) are given by :

$$p_{\perp} = \sqrt{p_x^2 + p_y^2} \quad (23)$$

$$\gamma_{\perp} = \sqrt{1 + p_{\perp}^2 / m_s^2 c^2} \quad (24)$$

$$\alpha = \frac{\gamma_{\perp}}{2} \sqrt{\Gamma_s / \Theta_s + i (\omega - k_z c) \tau'} \quad (25)$$

$$\beta = \frac{\gamma_{\perp}}{2} \sqrt{\Gamma_s / \Theta_s + i (\omega + k_z c) \tau'} \quad (26)$$

The integrals (22a)-(22f) were first derived by Trubnikov [21]. Note also that the above integrals are computed assuming a relativistic Maxwellian distribution function. The analytical integration over p_z leads to expressions involving modified Bessel functions K_n . In the general case of non-Maxwellian distribution functions, an analytical integration over p_z might not be possible, in which case it would have to be performed numerically as for the $p_{x,y}$ components. This will of course decrease the speed of computation of the dispersion relation.

4. The eigenvalue system

4.1. Derivation

The eigenvalue system is found by solving the equations for the electromagnetic potential determined according to the source distribution given by (19a), (19b), (19c) and (19d). Inserting the latter expressions into (7a) and (7b), the eigenvalue system reads :

$$\phi''(x) - \left(k^2 - \frac{\omega^2}{c^2} \right) \phi(x) + \frac{\rho(x)}{\varepsilon_0} = 0 \quad (27a)$$

$$\vec{A}''(x) - \left(k^2 - \frac{\omega^2}{c^2} \right) \vec{A}(x) + \mu_0 \vec{j}(x) = 0 \quad (27b)$$

where prime ' denotes derivative with respect to x . The set of equations (27a) and (27b) can be written in terms of the unknown 4-dimensional vector $\vec{\Psi} = (\phi, \vec{A})$

$$M(\omega, \vec{k}) \cdot \vec{\Psi} = 0 \quad (28)$$

It is a *non-linear* eigenvalue problem for the matrix M with eigenvector $\vec{\Psi}$ and eigenvalue ω . Daughton [4] solved this system by locating the zeroes of the determinant of M . We modify his method slightly by solving simultaneously for both the eigenvalues and the eigenvectors. A Newton-Raphson algorithm is used to find ω and $\vec{\Psi}$. To check if the matrix M is singular, or in other words, if the iteration process has converged, instead of computing the determinant of M , which should vanish, we attempt to zero the ratio between the smallest and largest of the eigenvalues λ_i of the matrix *linear* eigenvalue equation $M \cdot \vec{u} = \lambda \vec{u}$. This latter eigenvalue equation should not be confused with our original initial physical eigenvalue problem (28) and is absolutely not related to the computation of the dispersion relation. This procedure of computing the eigenvalues λ of M is simply another mean to verify if M is singular. It helps to decide whether the algorithm has converged or not. More details are given in the next subsection. This procedure allows us to track the dispersion curves through crossing points. An example is given below.

4.2. Algorithm

Finding the roots of the determinant of the matrix M is the traditional way to search for the *non-linear* eigenvalues in (28). However, it is not the method of choice in our problem because of the existence of different branches of the dispersion relation. For multiple branches in the dispersion relation, it is more efficient to look simultaneously for the eigenvalues and the eigenvectors.

As an example, consider a homogeneous plasma (extension to an inhomogeneous configuration is straightforward). In this case, the matrix M is of dimension 4×4 , and $\vec{\Psi}$ has 4 components, one for ϕ and three for \vec{A} , each of which is complex.

At this stage there are 10 unknowns:

- the complex eigenvalue ω (real and imaginary parts) ;
- the complex eigenfunction $\vec{\Psi}$ (real and imaginary parts each of the 4 components).

We first reduce the system by normalising the eigenvector to unity, $||\vec{\Psi}|| = 1$ and by setting its phase such that the imaginary part of the last component of $\vec{\Psi}$ vanishes, which we refer to as phase locking. The remaining 8 independent unknowns must then be found by solving the nonlinear system (28), that consist of 8 equations. To do this, we use the standard, globally convergent Newton-Raphson method, [22].

For fixed \vec{k} , the iteration starts with an initial guess for the eigenvalue $\omega = \omega_0$ and the eigenvector $\vec{\Psi} = \vec{\Psi}_0$. An improved guess is found by Newton-Raphson iteration in 8 dimensions. Each step involves evaluating the Jacobian of the system (28) and uses line searches and backtracking as described in [22]. The iteration is stopped when the matrix M is close to being singular, i.e. when $\det M \approx 0$. This condition is verified

indirectly by computing the four complex eigenvalues of M , $(\lambda_1, \lambda_2, \lambda_3, \lambda_4)$, that are solutions of the *linear* eigenvalue problem $M \cdot \vec{u} = \lambda \vec{u}$. We emphasize that the λ_i should not be confused with the eigenvalues ω of our original *nonlinear* problem. When the ratio of the smallest to the largest λ_i is sufficiently small, namely when

$$\frac{\min_{i \in [1..4]} \|\lambda_i\|}{\max_{i \in [1..4]} \|\lambda_i\|} < \varepsilon \quad (29)$$

with, typically, $\varepsilon = 10^{-6} \dots 10^{-8}$, we assume that convergence has been achieved and terminate the iteration procedure.

5. Results

We apply our algorithm to the following cases :

- the familiar electromagnetic oscillation modes of a nonrelativistic magnetised plasma ;
- a counter-streaming pair-plasma with nonrelativistic temperature and nonrelativistic drift speed corresponding to two oppositely shifted Maxwellian distribution functions ;
- a counter-streaming pair plasma with relativistic temperature and drift speeds close to the velocity of light, $U_s = 0.05 - 0.3 c$.

5.1. Plasma oscillations

The dispersion relation for a single species plasma in a homogeneous magnetic field obtained using a nonrelativistic version of our code is shown in figure 1. The plasma frequency is normalised to unity $\omega_p = 1$ and the thermal speed of the non-relativistic Maxwellian is $v_{th} = 0.1 c$. In figure 1, we compare our numerical results with the analytic expressions found using a simple root finding algorithm from the exact dispersion relation for wave propagation parallel to the magnetic field \vec{B}_0 , ($k_y = 0$) in order to check the correctness of our algorithm implementation. For electrostatic waves, we found the usual dispersion relation

$$1 + 2 \frac{\omega_p^2}{k_z^2 v_{th}^2} \left[1 + \frac{\omega}{k_z v_{th}} Z \left(\frac{\omega}{k_z v_{th}} \right) \right] = 0 \quad (30)$$

where the plasma dispersion function Z is defined for $\text{Im}(\zeta) > 0$ by

$$Z(\zeta) = \frac{1}{\sqrt{\pi}} \int_{-\infty}^{+\infty} \frac{e^{-t^2}}{t - \zeta} dt \quad (31)$$

and analytically continued for $\text{Im}(\zeta) < 0$, see for instance Delcroix and Bers [23]. For the left and right-handed circularly polarised electromagnetic wave we found

$$\frac{k_z^2 c^2}{\omega^2} = 1 + \frac{\omega_p^2}{\omega k_z v_{th}} Z \left(\frac{\omega \pm \omega_B}{k_z v_{th}} \right) \quad (32)$$

The numerical results are compared with the analytical exact expression for electrostatic waves (green curve, (30)) and electromagnetic waves (red and blue curves,

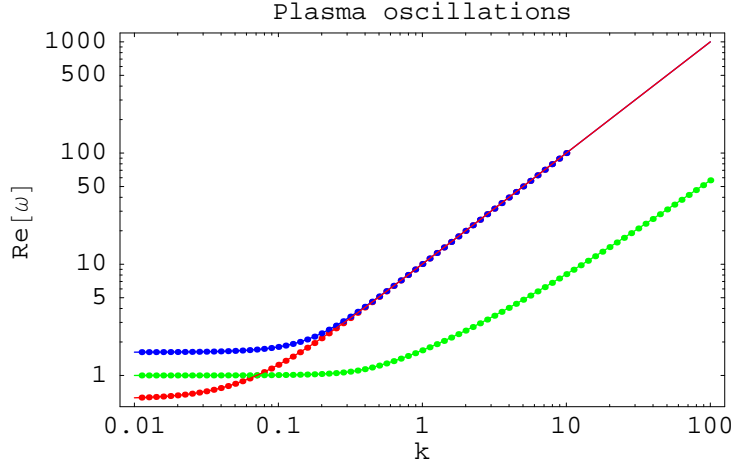


Figure 1. Dispersion relation for the transverse and longitudinal modes in a non-relativistic magnetised plasma. The exact analytical expressions for electrostatic waves are shown in green curve and those for electromagnetic waves are shown in red and blue curves. The plasma frequency is normalised to unity.

(32)). The advantages of implementing our modified root finding algorithm by looking for eigenvalues simultaneously with eigenfunctions is evident. The algorithm has no difficulty tracking only one branch of the dispersion relation even when crossing another branch. However it requires more computational effort since the root finding occurs in a space of higher dimension than is needed to find the eigenvalue alone.

To test our algorithm in cases where the imaginary part $\text{Im}(\omega)$ is small compared to the real part $\text{Re}(\omega)$, we consider electrostatic plasma oscillations, in the short wavelength limit, $k \ll 1$. Numerical results for $(\text{Re}/\text{Im})(\omega)$, respectively red and blue dots, are compared with the analytical dispersion relation, solid black curves, (30), figure 2. As long as the ratio $\text{Im}(\omega)/\text{Re}(\omega)$ is larger than the accuracy, which is about 5 digits, the results are reliable.

5.2. “Classical” Weibel instability

Next we check our algorithm for a situation with two counter-streaming species of non-relativistic temperature, taking $v_{\text{th}}/c = 10^{-3}$ and a small drift speed, $U_s = 0.1 c$.

We recall that the exact analytical dispersion relation for the classical counter-streaming Weibel instability for equal and opposite drift speed for both species with the same plasma frequency ω_p is given by

$$1 - \frac{k_z^2 c^2}{\omega^2} - 2 \frac{\omega_p^2}{\omega^2} \left[1 - \left(1 + 2 \frac{U_s^2}{v_{\text{th}}^2} \right) \left(1 + \frac{\omega}{k_z v_{\text{th}}} Z \left(\frac{\omega}{k_z v_{\text{th}}} \right) \right) \right] = 0 \quad (33)$$

The results are adapted from Delcroix and Bers [23]. In figure 3 we show the dispersion relation for the Weibel instability (red points) compared with the analytical expression (blue curve, (33)) and the asymptotic matching in case of a zero temperature plasma (green lines). The agreement is excellent.

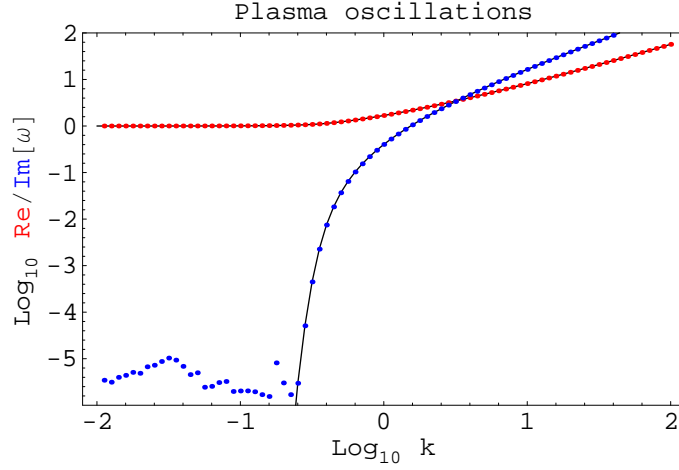


Figure 2. Dispersion relation for electrostatic plasma waves. The real and imaginary parts of the eigenfrequency are shown in red and blue dots respectively. The plasma frequency is normalised to unity.

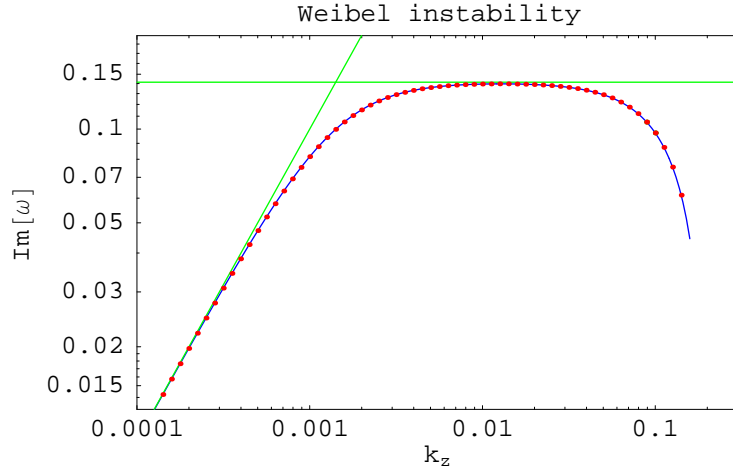


Figure 3. Growth rate for the non-relativistic Weibel instability ($\Theta_s \ll 1$). Results from our algorithm are depicted with red points, the exact analytical expression in blue curve and the asymptotic matching in case of a zero temperature plasma ($\Theta_s = 0$) in green lines.

Results for the dispersion relation in the case of small drift speeds are also shown in figure 4. Here, the large k_z asymptote is absent due to thermal effects.

5.3. Relativistic Weibel instability

Finally we computed the dispersion relation for a two-component fully relativistic counter-streaming plasma with high temperature, $\Theta_s = 10^2$ and different drift speeds as shown in figure 5. The dispersion curves are similar to those obtained in the classical Weibel instability. Due to the spread in momentum present at finite temperature, the instability is suppressed for large wavenumbers k_z in both the classical and relativistic cases.

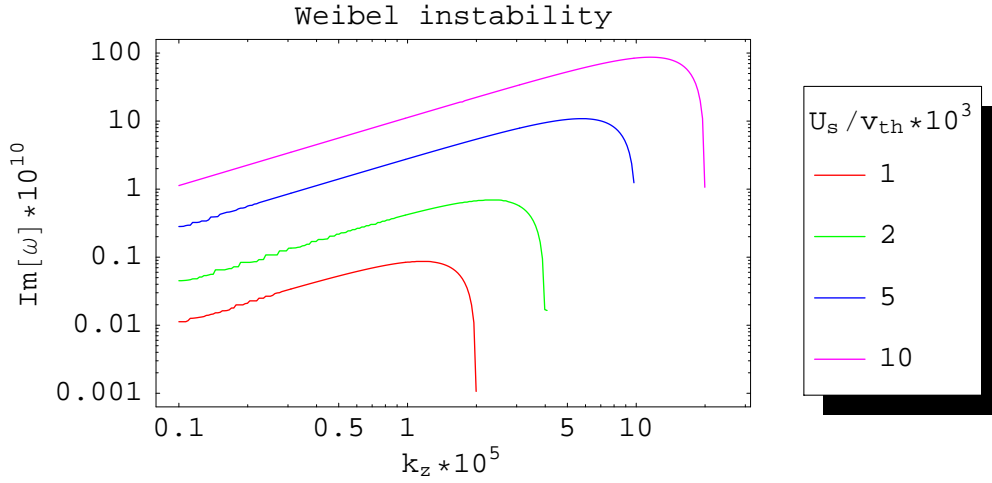


Figure 4. Growth rate for the non-relativistic Weibel instability ($\Theta_s \ll 1$) for different drift speeds U_s .

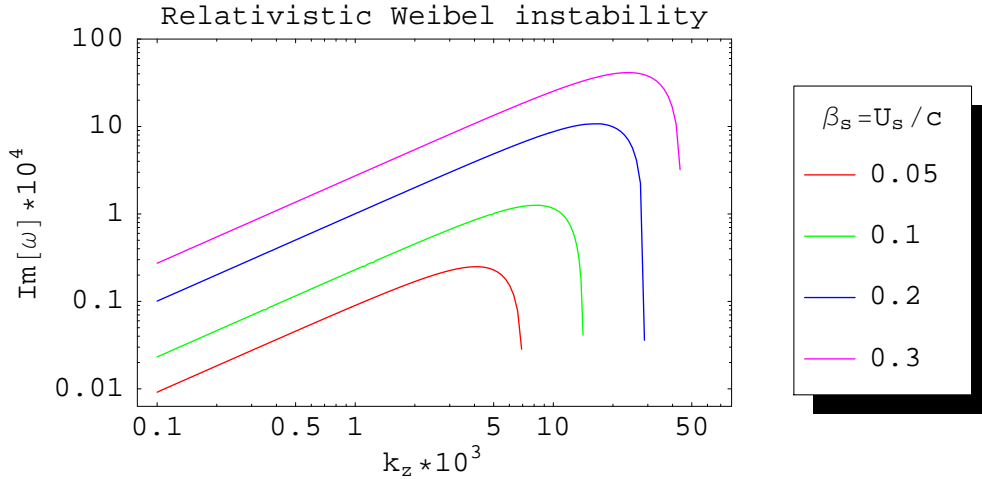


Figure 5. Growth rate for the relativistic Weibel instability ($\Theta_s \gg 1$) for different relativistic drift speeds U_s .

6. Conclusion

We have constructed an algorithm to solve the dispersion relation for non-relativistic and relativistic multi-component plasmas. The code has been validated by comparing the results with some typical configurations with homogeneous magnetic field, for which the analytical dispersion relation is known. New results have been obtained for the growth rate of the relativistic Weibel or two-stream instability for two counter-streaming relativistic Maxwellians which complement those found using a water-bag distribution. This code is easily extended to inhomogeneous plasmas, and is therefore a suitable tool for the study of stability properties of configurations of interest in gamma-ray burst and pulsar wind theories.

Acknowledgments

This research was supported by a grant from the G.I.F., the German-Israeli Foundation for Scientific Research and Development.

References

- [1] T. Piran. The physics of gamma-ray bursts. *Reviews of Modern Physics*, 76:1143–1210, 2005.
- [2] F. C. Michel. Winds from Pulsars. In *Revista Mexicana de Astronomia y Astrofisica Conference Series*, pages 27–34, October 2005.
- [3] J. G. Kirk. Relativistic plasmas in pulsar winds. *Plasma Physics and Controlled Fusion*, 47:B719–B726, December 2005.
- [4] W. Daughton. The unstable eigenmodes of a neutral sheet. *Physics of Plasmas*, 6:1329–1343, April 1999.
- [5] E. S. Weibel. Spontaneously Growing Transverse Waves in a Plasma Due to an Anisotropic Velocity Distribution. *Physical Review Letters*, 2:83–84, February 1959.
- [6] P. H. Yoon and R. C. Davidson. Exact analytical model of the classical Weibel instability in a relativistic anisotropic plasma. *Physical Review A*, 35:2718–2721, March 1987.
- [7] P. H. Yoon. Electromagnetic Weibel instability in a fully relativistic bi-Maxwellian plasma. *Physics of Fluids B*, 1:1336–1338, June 1989.
- [8] L. O. Silva, R. A. Fonseca, J. W. Tonge, W. B. Mori, and J. M. Dawson. On the role of the purely transverse Weibel instability in fast ignitor scenarios. *Physics of Plasmas*, 9:2458–+, June 2002.
- [9] J. Wiersma and A. Achterberg. Magnetic field generation in relativistic shocks. An early end of the exponential Weibel instability in electron-proton plasmas. *A&A*, 428:365–371, December 2004.
- [10] Y. Lyubarsky and D. Eichler. Are Gamma-Ray Burst Shocks Mediated by the Weibel Instability? *ApJ*, 647:1250–1254, August 2006.
- [11] T.-Y. B. Yang, Y. Gallant, J. Arons, and A. B. Langdon. Weibel instability in relativistically hot magnetized electron-positron plasmas. *Physics of Fluids B*, 5:3369–3387, September 1993.
- [12] D. B. Melrose. Covariant description of dispersion in a relativistic thermal electron gas. *Australian Journal of Physics*, 35:41–+, 1982.
- [13] R. Schlickeiser. Covariant kinetic dispersion theory of linear waves in anisotropic plasmas. I. General dispersion relation, bi-Maxwellian distribution and non relativistic limits. *Physics of Plasmas*, 11:5532–+, December 2004.
- [14] U. Schaefer-Rolfs and R. Schlickeiser. The relativistic kinetic Weibel instability: General arguments and specific illustrations. *Physics of Plasmas*, 13:2107, 2006.
- [15] R. C. Tautz and R. Schlickeiser. Counterstreaming magnetized plasmas. I. Parallel wave propagation. *Physics of Plasmas*, 12:2901–+, December 2005.
- [16] R. C. Tautz and R. Schlickeiser. Counterstreaming magnetized plasmas. II. Perpendicular wave propagation. *Physics of Plasmas*, 13:2901–+, June 2006.
- [17] I. Silin, J. Büchner, and L. Zelenyi. Instabilities of collisionless current sheets: Theory and simulations. *Physics of Plasmas*, 9:1104–+, April 2002.
- [18] B. Buti. Superluminous Waves in Streaming Relativistic Plasmas. *Physical Review A*, 1:1772–1774, June 1970.
- [19] B. Buti. Streaming Instabilities in Relativistic Magnetoplasmas. *Physical Review A*, 5:1558–1563, March 1972.
- [20] L. M. Zelenyi and V. V. Krasnoselskikh. Relativistic Modes of Tearing Instability in a Background Plasma. *Soviet Astronomy*, 23:460–+, August 1979.
- [21] B. A. Trubnikov. *Magnetic Emission of High Temperature Plasma*. PhD thesis, Dissertation, Moscow (US-AEC Tech. Inf. Service, AEC-tr-4073 [1960]), (1958), 1958.

- [22] W. H. Press, S. A. Teukolsky, W. T. Vetterling, and B. P. Flannery. *Numerical recipes in C. The art of scientific computing*. Cambridge: University Press, —c1992, 2nd ed., 1992.
- [23] J.L. Delcroix and A. Bers. *Physique des plasmas - Tome 2*. EDP Sciences - CNRS Editions, 1994.